Nanoscale

Accepted Manuscript

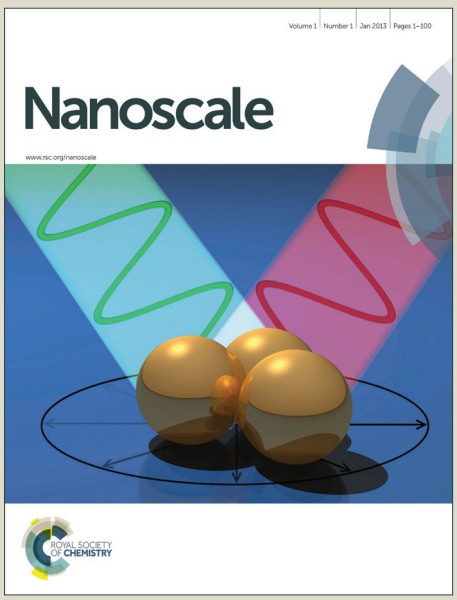

This is an *Accepted Manuscript*, which has been through the Royal Society of Chemistry peer review process and has been accepted for publication.

Accepted Manuscripts are published online shortly after acceptance, before technical editing, formatting and proof reading. Using this free service, authors can make their results available to the community, in citable form, before we publish the edited article. We will replace this *Accepted Manuscript* with the edited and formatted *Advance Article* as soon as it is available.

You can find more information about *Accepted Manuscripts* in the Information for Authors.

Please note that technical editing may introduce minor changes to the text and/or graphics, which may alter content. The journal's standard Terms & Conditions and the Ethical guidelines still apply. In no event shall the Royal Society of Chemistry be held responsible for any errors or omissions in this *Accepted Manuscript* or any consequences arising from the use of any information it contains.

ROYAL SOCIETY OF CHEMISTRY

www.rsc.org/nanoscale

Cite this: DOI: 10.1039/c0xx00000x

www.rsc.org/xxxxxx

ARTICLE TYPE

Lysozyme-Directed Synthesis of Platinum Nanoclusters as a MimicOxidase

Cheng-Ju Yu,[a]Tzu-Heng Chen,[a]Jhih-Yu Jiang,[a] and Wei-Lung Tseng*[a, b]

Received (in XXX, XXX) XthXXXXXXXXX 20XX, Accepted Xth XXXXXXXXX 20XX
DOI: 10.1039/b000000x

We present a simple, one-pot approach for synthesizing ultrafine platinum (Pt) nanoclusters (NCs) under alkaline conditions using lysozyme (Lys) as a template. From the analysis of them by matrix-assisted laser desorption/ionization time-of-flight mass spectrometry, Lys VI-stabilized Pt NCs majorly consisted of Pt_4 clusters. The formation of Pt NCs was confirmed using X-ray photoelectron spectroscopy and Fourier-transformed infrared spectroscopy. The maximal fluorescence of Pt NCs appears at 434 nm with a quantum yield of 0.08, a fluorescence lifetime of 3.0 ns, and excitation-dependent emission wavelength behavior. Pt NCs exhibit an intrinsic oxidase-like activity because Pt NC can catalyze O_2 oxidation of organic substrates through four-electron reduction process. Compared with larger Pt nanoparticles, the Pt NCs produce substantially greater catalytic activity in the O_2-mediated oxidation of 2,2'-azino-bis(3-ethylbenzothiazoline-6-sulphonic acid), 3,3',5,5'-tetramethylbenzidine, and dopamine.

1 Introduction

Molecule-like metal-based (Au, Ag, and Pt) nanoclusters (NCs), comprising several to tens of atoms, have attracted a considerable amount of attentionin the fields of heavy metal and biomolecule sensing, catalysis, biological imaging and labeling, and fuel cells.[1, 2]Compared to metal nanoparticles (NPs) with diameters greater than 2 nm, NCs exhibit greater catalytic activities and have discrete electronic structures.[3] A high percentage of the metal content of metal NCs is exposed to the nanoparticle surface. For example, in a 2.0-nm NC, 50% of the metal atoms are exposed. Consequently, metal NCs are highly active catalysts for several crucial reactions; Au NCs have been shown to catalyze the oxidation of carbon monoxide,[4, 5] the reduction of 4-nitrophenol,[6] and the reduction of oxygen.[7] Pt NCs exhibit extraordinarily high levels of activity in oxidizing carbon monoxide,[8] the reducing oxygen,[9] and oxidatively dehydrogenating propane.[10] Metal NPs, including Pt, Au, and Ag NPs, often exhibit peroxidase- and oxidase-like activities, and can catalyze the H_2O_2-mediated oxidation of peroxidase substrates, the oxidation of glucose with co-substrate O_2, and the oxidation of 2,2'-azino-bis(3-ethylbenzothiazoline-6-sulphonic acid) (ABTS) and 3,3',5,5'-tetramethylbenzidine (TMB) in the presence of O_2.[11-15]Au NCs exhibit peroxidase-like activity, and can catalyze the oxidation of TMB in the presence of H_2O_2.[16] However, few studies have reported using metal NCs to mimic oxidase.

Although these NCs do not possess plasmonic properties, they interact with light and undergo electronic transitions between discrete energy levels. The emission wavelength of metal NCs is tunable from the near-infrared to ultraviolet (UV) regions by changing the number of metal atoms that are present within the clusters.[17] For example, poly(amidoamine) dendrimer-encapsulated Au_5, Au_8, Au_{13}, Au_{23}, and Au_{31} clusters produce UV, blue, green, red, and near-IR emissions, respectively.[18] Moreover, Ag NCs with core sizes ranging from Ag_2 to Ag_8 emit over a range of 400 to 600 nm.[19, 20] However, in all of the metal NCs, relatively few studies have been devoted to the preparation of fluorescent Pt NCs. Kawasaki et al. proposed a one-pot, surfactant-free approach for synthesizing fluorescent Pt NCs with 4 to 6 Pt atoms in a *N,N*-dimethylformamide solution without capping ligands.[21] Poly(amidoamine) dendrimers with terminating hydroxyl groups were used as templates to direct the growth of fluorescent Pt_5 clusters and non-fluorescent Pt NPs by reducing H_2PtCl_6 with $NaBH_4$.[22] In another approach, a two-step process was developed to synthesize Pt NCs. First, nanometer-sized Pt particles were prepared by reducing H_2PtCl_6 with $NaBH_4$ in the presence of a capping agent, mercaptosuccinic acid.[23] The formed Pt particles were then etched to form Pt NCs by ligand exchange between the capping ligand and glutathione (GSH) on ã □ ã È-摧□LÃ È┬摧缺 ðÈ¶ reaction times, produce bulky Pt NPs, require the use of toxic organic solvents, and require multiple steps.

Lysozyme (Lys) can act as both a reducing and stabilizing agent in producing a wide variety of NPs, including Au,[24] Ag,[25] Si,[26] and TiO_2-based NPs.[26] Recently, Lys was successfully used as a template for synthesizing Au NCs. The resulting Lys-stabilized Au NCs were shown to inhibit bacterial growth,[27] detect Hg(II) and $CH_3Hg(I)$,[28] sense GSH,[29] and catalyze H_2O_2-mediated oxidation of TMB in the presence of graphene.[30] We

Yu, C.-J. and Chen, T.-H. contributed equally to the work

[a]*Department of Chemistry, National SunYat-sen University, Kaohsiung,Taiwan.Fax: 011-886-7-3684046; E-mail: tsengwl@mail.nsysu.edu.tw*

[b]*School of Pharmacy, College of Pharmacy, Kaohsiung Medical University, Taiwan. Fax: 011-886-7-3684046; E-mail: tsengwl@mail.nsysu.edu.tw*

† Electronic Supplementary Information (ESI) available: Experimentalprocedures on prepared compounds and Fig. S1-S16]. See DOI: 10.1039/b000000x/

Nanoscale Accepted Manuscript

report a one-pot synthesis of fluorescent Pt NCs through the reduction of H_2PtCl_6 with Lys at a low temperature (37 °C). The as-prepared fluorescent Pt NCs produce an intense blue emission at 437 nm, and in the presence of dissolved O_2, exhibit oxidase-like activity to oxidize ABTS, TMB, and dopamine.

2 Materials and methods

Materials

Lys (chicken eggwhite) was purchased from MP Biomedicals (Irvine, CA). $H_2PtCl_6{\cdot}6H_2O$, $FeCl_3.6H_2O$, $FeCl_2.4H_2O$, $HAuCl_4{\cdot}3H_2O$, $NaBH_4Na_2HPO_4$, NaH_2PO_4, NaCl, dopamine, ABTS, TMB, methylene blue, sodium acetate, sodium citrate, catalase (9473 units/mg, from Aspergillusniger), horseradish peroxidase (HRP; 50~150 units/mg), andα-cyano-4-hydroxycinnamic acid were ordered from Sigma-Aldrich (St. Louis, MO). Milli-Q ultrapure water (Milli-pore, Hamburg, Germany) was used in all of the experiments.

Characterization of Pt NCs

Absorption, fluorescence, and Fourier-transformed infrared spectroscopy (FT-IR) spectra of the Pt NCs were measured usinga double-beam UV-visible spectrometer (Cintra 10e, GBC, Victoria, Australia), a Hitachi F-7000 fluorometer (Hitachi, Tokyo, Japan), and a Nicolet 6700 FT-IR spectrometer (Thermo electron Corporation, Madison, WI) respectively. Time-resolved fluorescence measurements were conducted on an OB920 single-photon counting fluorometer (Edinburgh Analytical Instruments) with a pulsed nanosecond nitrogen lamp as excitation source. The elemental compositions of the Pt NCs were obtained using JAMP-9500F auger electron spectroscopy (JEOL, Japan).Matrix-assisted laser desorption/ionization time-of-flight mass spectrometry (MALDI-TOF MS) (BrukerDaltonics, Germany) was performed to determine the molecular weight of the Pt NCs. Prior to MALDI-TOF MS measurement, we mixed saturated α-cyano-4-hydroxycinnamic acid containing 70% acetonitrile with an equal volume of the purified Pt NCs and pipetted the resulting mixture onto a stainless steel 384-well target (BrukerDaltonics, Germany). In positive ion and reflectron mode, each final mass spectrum was accumulated as an average of 2000 single shot spectra. Laser fluence was set to 72 μJ/100 μm^2. Transmission electron microscopy (TEM) (JEM-1400; JEOL, Tokyo, Japan) was used to measure the size and composition of the Fe_3O_4, Pt, and Au NPs.

Preparation of Pt NCs, Pt NPs, Au NPs, and Fe_3O_4 NPs

The preparation of the Pt NCs was performed by chemical reduction of $H_2PtCl_6$with Lys, as a soft template.A solution of Lys (5 mL, 1–25 mg/mL) reacted with an equal volume of 10 mMH_2PtCl_6. The mixture was vigorously stirred for 2 min, followed by the rapid addition of NaOH (500 μL, 1 M). The obtained solution was incubated at 37°C overnight.To remove excess Lys, a solution of Pt NCs was dialysed with 5 mM phosphate buffer (pH 3) for two day. The concentration of the obtained Pt NCs is denoted as 1×. The preparation of Pt NPs (5 ± 2 nm and 30 ± 4 nm), Au NPs (13 ± 2 nm), and Fe_3O_4 NPs (13 ± 2 nm) was described in the supporting information.

Pt NCs-induced oxidation reaction

Stock solutions of ABTS, TMB, and dopamine were prepared in deionized water. Pt NCs (50 μL, 1×) were added to a solution consisting of ABTS (100 μL, 1 mM), deionized water (350 μL), and acetate (500 μL, 100 mM; pH 2.0–6.0). The pH of acetate solution was adjusted by adding NaOH or HCl. The mixture was incubated at ambient temperature for 0–60 min. The absorption spectra of the mixture were collected using a visible spectrophotometer. Under the same reaction conditions, TMB and dopamine were used instead of ABTS, once at a time. To study the steady-state mechanism of Pt NC-induced oxidation reaction, variable concentrations of TMB (0.1–1 mM) was used as substrates while the concentration of the Pt NCs (0.05×) was kept constant. The zero order rate constants were obtained from linear plotting of the maximal absorbance versus time. Steady-state kinetic assays were carried out in 50 mM sodium acetate (pH 3.0). The kinetic parameter, V_{max} and K_m, were calculated according to the Michaelis-Menten equation.

3 Results and Discussion

Synthesis and Characterization of Pt NCs

The preparation of Pt NCs was conducted prepared by reducing H_2PtCl_6 with Lys under basic conditions at 37 °C for 12 h. When the concentration of Lys varied from 1 to 25 mg/mLat a fixed concentration of H_2PtCl_6 (10 mM), the reaction of H_2PtCl_6 with 5 mg/mL (approximately 0.35 mM) Lys showed the most intense fluorescence intensity at 434 nm (**Fig. S1**, ESI).At the Lys concentrations of 1 and 2 mg/mL, the formed Pt NCs exhibited weaker fluorescence as a result of the production of large-sized Pt NCs. Similar phenomena were observed when bovine serum albumin (BSA) and Lys were used to prepare BSA- and Lys-stabilized AuNCs, respectively.[28, 31]In the concentration range of 10–25 mg/mL Lys, the fluorescence of the as-prepared Pt NCs progressively decreased with increasing Lys concentrations. This is probably due to the fact that a large amount of the precursor was consumed in the formation of nuclei, resulting in a decrease in the formation of Pt NCs. We suggest that the role of Lys is to act as the sole reducing agent. Thus, a high molar ratio of Lys to H_2PtCl_6 facilitates the formation of Pt NCs, while a low molar ratio of Lys to H_2PtCl_6 induces the production of Pt NPs and Pt NCs. Taken together, 5 mg/mL was selected for the subsequent study. Because the size of the resulting Pt NCs was too small to be observed in standard TEM.[1] Thus, MALDI-TOF MS was used to determine the size of the metal NCs[1] and confirm the production of Pt NCs. The molecular weight of Lys was determined to be 14.3 kDa by using MADLI-TOF MS (**Fig. 1A**). When Lys was incubated with a solution of H_2PtCl_6, the resulting solution was immediately detected using MALDI-TOF-MS. **Fig. S2 (ESI)** shows that the formation of Au^+–Lys complexes caused a shift in molecular mass. Compared to Lys and Au^+–Lys complexes, the MALDI-TOF MS spectrum for Lys-stabilized Pt NCs consisted of several peaks between *m*/*z*

Nanoscale Accepted Manuscript

This journal is © The Royal Society of Chemistry [year]

14000 and 16000 (**Fig. 1B**). One of these peaks appearing at 14318 was assigned to $[Lys + H]^+$, while other peaks with an average *m*/*z* of 15098 corresponded to different sizes of Lys-stabilized Pt NCs. According to the difference in *m*/*z* value between the above average peak and Lys peak, the average number of Pt atoms in Lys-stabilized Pt NCs is 4. This signifies that Pt_4 clusters are major products in a mixture of Pt NCs. This result also reflects that Lys may remain bound to Pt NCs during the MALDI-TOF MS process. Similar phenomena occurred during the MALDI-TOF MS analysis of protein-stabilized Au_8 and Au_{25} clusters.[29, 31, 32] Differences in the molecular weights of Lys and Lys-stabilized Pt provide clear evidence for the formation of Pt NCs. X-ray photoelectron spectroscopy (XPS) was used to determine the valence state of Pt NCs. The XPS spectrum of dried Pt NCs revealed a peak indicative of Pt $4f_{7/2}$ at 71.7 eV, which differs from the reported XPS peaks for $PtCl_4$, $PtCl_2$, and bulk Pt, which appear at 75.0, 73.2, and 70.9 eV, respectively (**Fig. 2**) [9].

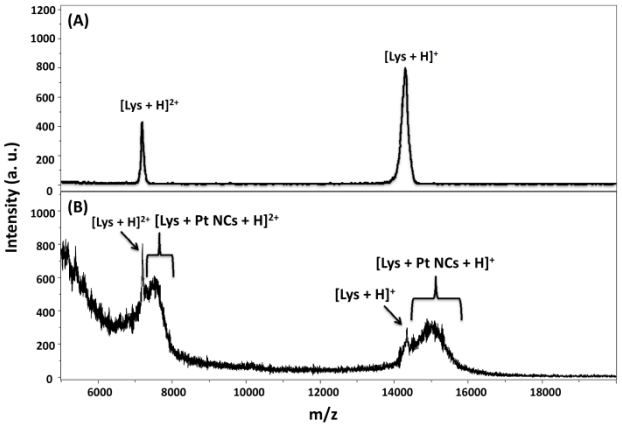

Fig. 1 MALDI-TOF mass spectra of (A) Lys and (B) Lys-stabilized Pt NCs

Moreover, the peak position of Pt $4f_{7/2}$ for Pt NCs appears between the Pt(0) and Pt(II) peak positions. Relative to the binding energy of bulk Pt, Pt NCs showed the positive shift in the Pt $4f_{7/2}$ peak position. This shift is attributed to the fact that the binding energy of metal clusters increases with reducing cluster size. The best fit of the data reveals that the Pt NCs contained approximately 67% Pt(I) and 33% Pt(0); there was no evidence for the presence of an oxidized precursor, $Pt(II)Cl_4^{2-}$. This is similar to the reported composition of glutathione-protected Pt NCs, which contained 90% Pt(I) and a complementary Pt(0) content.[23] Lin and Tseng reported that Hg^{2+} induces fluorescence quenching of Au_{25} clusters through the formation of metallophilic bonds between Hg(II) ($4f^{14}5d^{10}$) and Au(I) ($4f^{14}5d^{10}$).[28] This effect could be applied to demonstrate the presence of Pt(0) in Pt NCs because Pt(0) ($4f^{14}5d^{10}$) can bind to Hg(II) through metallophilic interactions.[33] **Fig. S3** (ESI) shows that fluorescence quenching of Pt NCs occurs when the Hg(II) ion is added, confirming the presence of Pt(0) in Pt NCs. FT-IR was used to examine the interactions between Lys and Pt NCs. The FT-IR spectrum of Lys contains two major bands at 1664 and 1543 cm^{-1}, which correspond to amide I (C=O stretching) and amide II (N-H bending coupled with C–N stretching) bonds, respectively (curve a in **Fig. S4**, ESI). By contrast, the FT-IR spectrum of Lys-stabilized Pt NCs shows less intense absorptions at 1664 and 1543 cm^{-1}, suggesting that there are fewer amide I and II bonds present because the occurrence of the Lys secondary structure decreased (curve b in **Fig. S4**, ESI**).** Comparing the Lys and Lys-stabilized Pt NC spectra reveals that the Lys amide I and II bonds are blue-shifted in the complex, suggesting that Pt NCs interact with the Lys peptide bonds. Sennuga et al. reported that the interaction between Pt NPs and apoferritin results in similar shifts in the amide I and II absorption bands.[34]

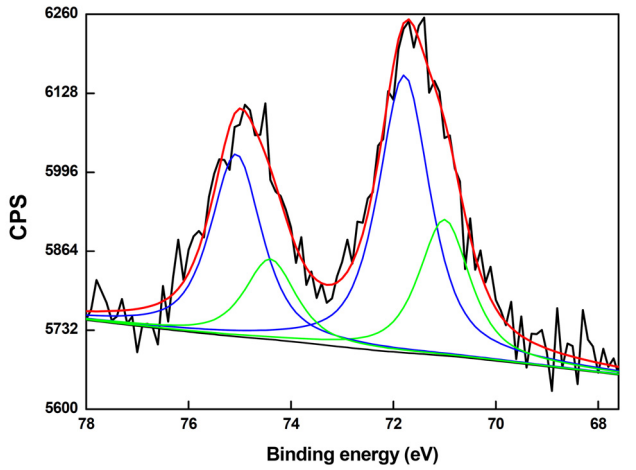

Fig. 2 X-ray photoelectron spectrum of Lys-stabilized Pt NCs. The original spectrum is in black, the fitted spectrum is in red, the Pt(I) $4f_{7/2}$ spectrum is in blue, and the Pt(0) $4f_{7/2}$ spectrum is in green.

Optical Properties and Stability of Pt NCs

In a solution,H_2PtCl_6 has an absorbance maximum at 260 nm (**Fig 3A**), which results from a ligand-to-metal charge transfer within the $[PtCl_6]^{2-}$ ions.[35] Following the addition of Lys to a solution of the $[PtCl_6]^{2-}$ ions, the absorbance intensity at 260 nm decreases (**Fig. 3A**), whereas the fluorescence gradually increases (**Fig. 3B**). After incubating overnight at 37 °C, the fluorescence intensity of a mixture of the $[PtCl_6]^{2-}$ complex ions and Lys was remarkably larger than that of Lys (**Fig. S5**, **ESI**). These results suggest that the observed blue emission arises from the Pt NCs, and not from Lys. Thus, a mixture of the $[PtCl_6]^{2-}$ complex ions and Lys progressively converted to Pt NCs over time. The maximal emission shifts to longer wavelengths when the excitation wavelength increases from 350 to 500 nm, suggesting that the as-prepared solution contains a mixture of Pt NCs with different particle sizes (**Fig. 3C**). When a long pass filter (475 nm cut-off filter) was used to block scattering from the excitation wavelength, we still observed that the maximal emission shifted from 510 to 556 nm by changing excitation wavelength from 425 to 465 nm (**Fig. S6, ESI**). We rule out that excitation-dependent change in spectra is due to scattering from Lys and Pt NCs. Thus,

Nanoscale Accepted Manuscript

excitation-dependent fluorescence behavior arises from different sized NCs in the as-prepared solution. Kawasaki et al. found that the maximal fluorescence emission wavelength for ligand-free Pt NCs increases when the excitation wavelength increases.[21] The most intense fluorescence emission occurs at 434 nm when the solution was excited at 370 nm, indicating that Pt_4 clusters are dominant in a mixture of Pt NCs, according to the spherical Jellium model:[36]

$$E_{Fermi}/N^{1/3}$$ (E_{Fermi} = 4.28 eV for Pt).

A tetrahedral geometry provides the lowest energy structure for Pt_4 clusters.[37] Using quinine sulfate as the reference, we estimated that the Pt NCs provide a quantum yield of 8% (**Fig. S7**, ESI). Numerically fitting the fluorescence at 434 nm (excitation at 370 nm) revealed a fluorescence lifetime of 3.0 ns for the blue-emitting Pt NCs (**Fig. 3D**). This short lifetime may originate from singlet transitions between the filled d- and sp-conduction bands. To demonstrate the formation of different sized Pt NCs, lifetime values of green-emitting Pt NCs were obtained by numerically fitting the fluorescence at 520 nm (excitation at 485 nm). **Fig. S8 (ESI)** shows that Pt NCs exhibited two lifetime of 5.4 (73%) and 36.1 ns (27%). We tested the stability of Pt NCs by monitoring their fluorescence in a 50-mM phosphate solution (pH 7.0) containing 0–400 mM NaCl (**Fig. S9**, ESI).The fluorescence remained constant for the range of test conditions, indicating that Pt NCs have potential for molecular sensing under physiological conditions.

Pt NCs Mimic Oxidase Activity

HRP catalyzes the H_2O_2-mediated oxidation of ABTS and TMB. These dyes have applications in bioassay, such as enzyme-linked immunosorbent assay (ELISA), and biosensing applications. Recently, NP-based materials, including Fe_3O_4 and Au NPs, were used in place of HRP because they offer greater resistance to denaturation and protease digestion and are simpler to prepare and store.[11,38,39] However, the peroxidase-catalyzed reactions require H_2O_2 as an electron acceptor. CeO_2 NPs, Pt nanodot-coated Au nanorods, and PdPt alloy nanodot-coated Au nanorods exhibit oxidase-like activity in the catalytic O_2 oxidation of ABTS and TMB.[40-42] Because the template-based direct synthesis of metal NCs does not require using stabilizing ligands, metal clusters located in templates can provide non-block, active surfaces for catalyzing chemical reactions.[1] We used Lys as a template for synthesizing Pt NCs and investigated whether

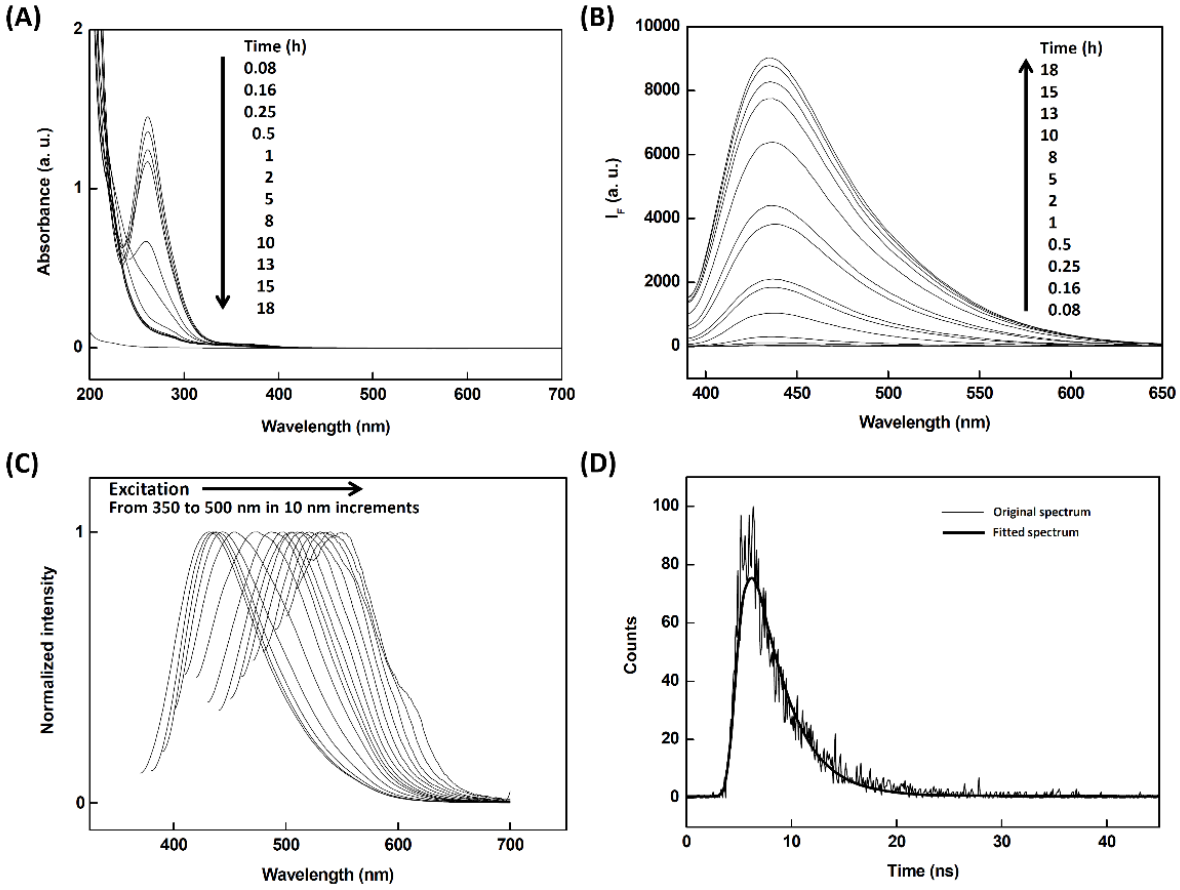

Fig. 3 (A) Absorption and (B) fluorescence spectra obtained from the synthesis of Pt NCs at different growth times. (C) Fluorescence spectra of Pt NCs with excitation of different wavelength. (D) Fluorescence lifetime decay of Pt NCs.

Nanoscale Accepted Manuscript

This journal is © The Royal Society of Chemistry [year]

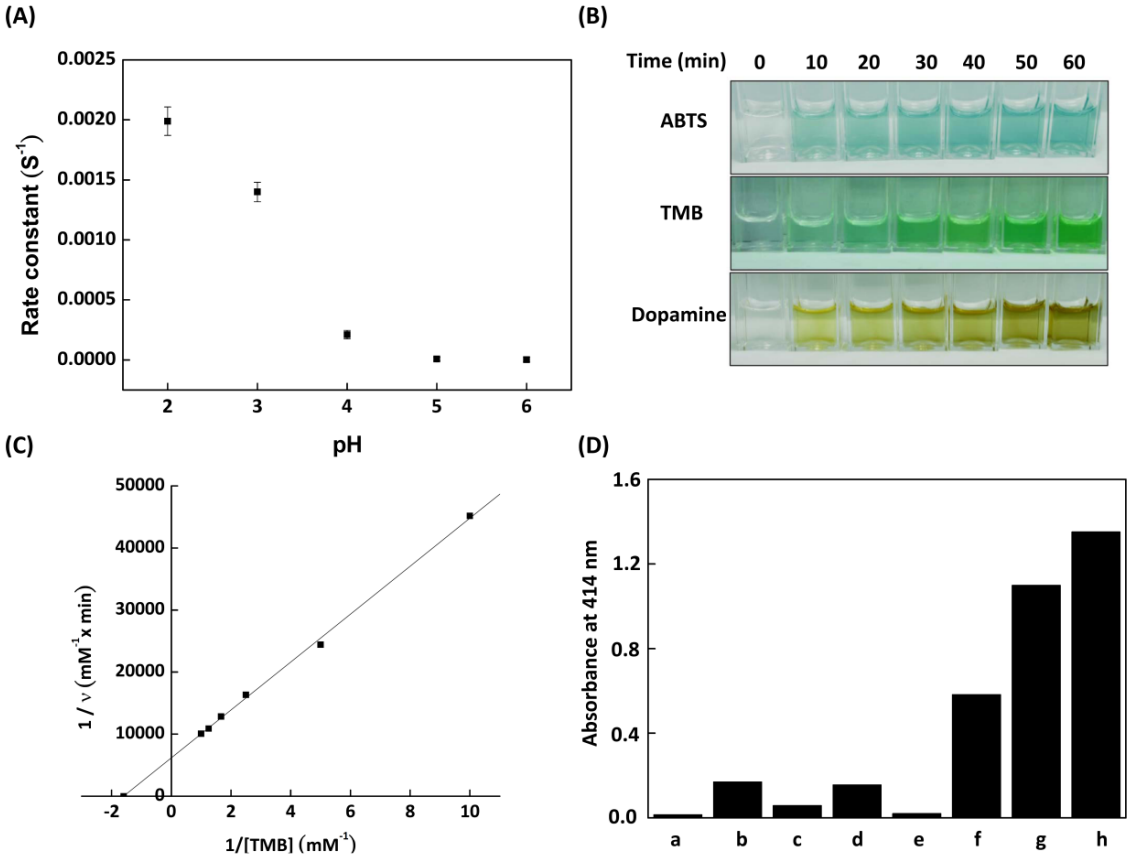

Fig. 4 (A) Effect of solution pH on the catalytic rate of Pt NCs. 0.05× Pt NCs were incubated with a solution containing 0.1 mM ABTS and 50 mM sodium acetate. (B) Photographs of colored product obtained from the reaction of 0.05× Pt NCs with 0.1 mM ABTS, 0.1 mM TMB, and 0.1 mM dopamine at pH 2.0, 3.0, and 7.0, respectively. (C) Double reciprocal plot of activity of Pt NCs with the constant concentration of Pt NCs. The velocity (ν) obtained from the incubation of Pt NCs with different concentration of TMB at pH 4.0. (D) The intensity of the absorbance at 414 nm of oxidized ABTS obtained in the absence (a) and presence of (b) Lys, (c) HRP, (d) 13 nm diameter Au NPs, (e) 13 nm diameter Fe_3O_4 NPs, (f) 30 nm diameter Pt NPs, (g) 5 nm diameter Pt NPs, and (h) Pt NCs. ABTS (0.1 mM, pH 2.0) was incubated with nanomaterial/protein at ambient temperature for 10 min. The concentration of each nanomaterial and protein was fixed at 5 mg/mL.

Lys-stabilized Pt NCs catalyze the oxidation of ABTS and TMB. Lys-stabilized Pt NCs were incubated with ABTS in 50 mM acetate solution at pH 2.0–6.0.**Fig. 4A and 4B** show the time-dependent absorbance at 414 nm and color changes of 0.1 mM ABTS following the addition of 0.05× Lys-stabilized Pt NCs to an ABTS solution with a pH ranging from 2.0 to 6.0.**Fig. S10** (ESI) shows their corresponding visible spectra. In the absence of H_2O_2, the maximal catalytic rate for Pt NC-catalyzed oxidation of ABTS was at pH 2.0. In the absence of Pt NCs, no oxidation of ABTS is apparent over the pH range of 2.0 to 6.0 (**Fig. S11**, ESI).Under the same concentration of Pt NCs, 0.1 mM TMB underwent Pt NC-induced oxidation and color change at acidic pH levels (**Fig. 4B**; **Fig. S12**, ESI). By monitoring the change in absorbance at 650 nm, the maximal catalytic rate for Pt NC-catalyzed one electron oxidation of TMB was at pH 3.0. This result is inconsistent with our prediction that the most rapid oxidation of TMB occurs at pH 2.0 in the presence of Pt NCs. This is probably attributed to the fact that Pt NCs catalyze two electron oxidation of TMBat pH 2.0, generating the oxidized TMB with an absorbance maximum at 450 nm.[43] We used dopamine to verify the Pt NCs oxidation properties because of its resistance to oxidation. Adding 0.05× Pt NCs to a solution of 0.1 mM dopamine at pH 7.0 caused the solution to change from colorless to orange (**Fig. 4B**) and the characteristic absorption bands in the UV-visible spectrum to emerge (**Fig. S13**, ESI). These changes are characteristic of dopamine conversion to aminochrome, a major oxidation product.[44] In the absence of Pt NCs, the UV-visible spectrum and color of the dopamine solution remain almost constant, even after days of incubation. Taken together, these results clearly demonstrate the intrinsic oxidase-like activity of Pt NCs. **Fig. 4C** shows that, at a pH of 4.0, the catalytic activity of Pt NCs toward the oxidation of TMB follows a Michaelis-Menten mechanism. The Michaelis constant (K_m) and maximal velocity (V_{max}) were determined to be 0.63 mM and 2.7 μM s^{-1}, respectively, by using the Michaelis-Menten equation. Compared to HRP- and Fe_3O_4 NP-catalyzed oxidation of TMB in the presence of H_2O_2,[38] Pt NCs provide a relatively small

Nanoscale Accepted Manuscript

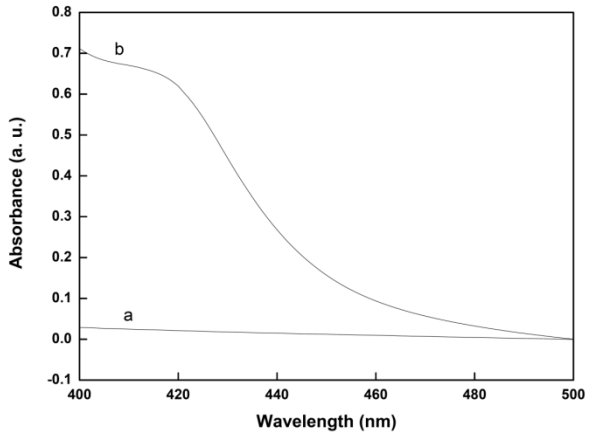

Fig. 5 Absorption spectra of a solution containing 0.1 mM ABTS, 0.05× Pt NCs and 50 mM sodium acetate (pH 2.0) under (a) N_2-saturated and (b) aerobic conditions.

value of K_m (high affinity for the substrate), and a relatively large value for V_{max}. This result clearly indicates that Pt_4 clusters provide higher catalyst efficiency even in the absence of H_2O_2. Additionally, in comparison with oxidase-like activity of CeO_2 NPs (size = 5–100 nm, K_m = 0.8–3.8mM, V_{max} = 0.3–0.7 μM s^{-1}),[40] Pt Ncs show lower K_m value and higher V_{max} value than CeO_2 NPs. In addition to examining Pt NCs, we investigated whether HRP, Lys, Fe_3O_4 NPs (13 ± 2 nm), Au NPs (13 ± 2 nm), Pt NPs (30 ± 4 nm), and Pt NPs (5 ± 1 nm) catalyze the oxidation of ABTS in the absence of H_2O_2. However, **Fig. 4D** reveals that only Pt NCs exhibited high performance in the catalytic oxidation of ABTS.

The catalytic oxidation of ABTS by Pt-based nanomaterials follows the trend Pt NCs > Pt NPs (5 nm) > Pt NPs (30 nm), suggesting that the catalytic activity of Pt-based nanomaterials is highly dependent on particle size. This is attributed to the fact that Pt NCs has a high surface area to volume ratio, thus providing more active sites for the catalysis of ABTS. This result also suggests that the use of a template did not block the active surfaces of metal clusters during catalysis. Previous studies have demonstrated that Pt NCs can efficiently catalyze the reduction of oxygen to water through a four-electron reduction reaction in electrocatalytic processes.[9, 45] He et al. coated Au nanorods with Pt nanodots and used them as oxidase mimetics for the catalytic oxidation of TMB through a four-electron process.[41] They suggested that Au-Pt nanostructures, dissolved O_2, and TMB served as a catalyst, an electron acceptor, and an electron donor, respectively. **Fig. 5** shows that the as-prepared Pt NCs cannot catalyze the oxidation of ABTS under N_2-staturated conditions, which indicates the importance of O_2 in the oxidation process. Because Pt NCs could reduce O_2 to H_2O_2 through a two-electron reduction process [$O_2(g)$ + $2H^+(aq)$+ $2e^- \rightarrow H_2O_2(aq)$] and then catalyze H_2O_2-mediated oxidation of organic substrate, catalase converting H_2O_2 into water was used to exclude this possibility. Because the absorption spectrum of oxidized ABTS overlaps that of catalase, TMB was used instead of ABTS. **Fig. S14** (ESI) shows that catalase rarely inhibited the Pt NC-catalyzed O_2 oxidation of TMB. According to previous studies and our present findings, we propose that the possible mechanism of Pt NC-catalyzed O_2 oxidation of organic substrates involves a four-electron reduction process [$O_2(g)$ + $4H^+(aq)$ + $4e^- \rightarrow$ $2H_2O(l)$]. Moreover, dissolved O_2 and ABTS act as an electron acceptor and an electron donor, respectively.These findings motivated us to apply Pt NCs to the oxidation of pollutants in environmental water. Following the addition of Pt NCs, the 665-nm maximal absorbance of methylene blue in lake water samples gradually decreased (**Fig. S15**, ESI). Pt NCs degrade methylene blue in a complex matrix in the absence of H_2O_2. By contrast, previous studies have reported that high concentrations of H_2O_2 are required for metal NP-induced degradation of environmental pollutants.[46]

Conclusions

This study has reported a straightforward one-pot approach to preparing blue-emitting and oxidase-like Pt NCs using Lys as a template at a pH of 12.0. This result is helpful to realize that protein can act as unique template for synthesizing not only Au and Ag NCs, but also Pt NCs. Lys-stabilized Pt NCs catalyze the O_2 oxidation of ABTS, TMB, and dopamine through a four-electron reduction process. We demonstrated the practical applicability of Lys-stabilized Pt NCs in degrading methylene blue in the absence of H_2O_2. We found that the fluorescence quenching of Pt NCs occurs in the presence of Hg(II) and Cu(II), and this is a subject requiring further investigation.

Acknowledgements

We would like to thank the National Science Council (NSC 100-2628-M-110-001-MY4) for the financial support of this study.

Notes and references

1. Y. Z. Lu and W. Chen, *Chem. Soc. Rev.*, 2012, **41**, 3594-3623.
2. S. J. Guo and E. K. Wang, *Nano Today*, 2011, **6**, 240-264.
3. J. Zheng, P. R. Nicovich and R. M. Dickson, *Annu Rev Phys Chem*, 2007, **58**, 409-431.
4. A. A. Herzing, C. J. Kiely, A. F. Carley, P. Landon and G. J. Hutchings, *Science*, 2008, **321**, 1331-1335.
5. A. Bongiorno and U. Landman, *Phys. Rev. Lett.*, 2005, **95**.
6. H. Yamamoto, H. Yano, H. Kouchi, Y. Obora, R. Arakawa and H. Kawasaki, *Nanoscale*, 2012, **4**, 4148-4154.
7. W. Chen and S. Chen, *Angew. Chem. Int. Ed.*, 2009, **48**, 4386-4389.
8. S. Dobrin, *Phys. Chem. Chem. Phys.*, 2012, **14**, 12122-12129.
9. K. Yamamoto, T. Imaoka, W. J. Chun, O. Enoki, H. Katoh, M. Takenaga and A. Sonoi, *Nat. Chem.*, 2009, **1**, 397-402.
10. S. Vajda, M. J. Pellin, J. P. Greeley, C. L. Marshall, L. A. Curtiss, G. A. Ballentine, J. W. Elam, S. Catillon-Mucherie, P. C. Redfern, F. Mehmood and P. Zapol, *Nat. Mater.*, 2009, **8**, 213-216.
11. W. Luo, C. Zhu, S. Su, D. Li, Y. He, Q. Huang and C. Fan, *ACS Nano*, 2010, **4**, 7451-7458.
12. M. Ma, Y. Zhang and N. Cu, *Colloids Surf., A*, 2011, **373**, 6-10.
13. Y. Jv, B. X. Li and R. Cao, *Chem. Commun.*, 2010, **46**, 8017-8019.
14. S. Wang, W. Chen, A. L. Liu, L. Hong, H. H. Deng and X. H. Lin, *Chemphyschem*, 2012, **13**, 1199-1204.
15. H. Jiang, Z. H. Chen, H. Y. Cao and Y. M. Huang, *Analyst*, 2012, **137**, 5560-5564.

Nanoscale Accepted Manuscript

This journal is © The Royal Society of Chemistry [year]

16. X. X. Wang, Q. Wu, Z. Shan and Q. M. Huang, *Biosens. Bioelectron.*, 2011, **26**, 3614-3619.
17. L. Shang, S. J. Dong and G. U. Nienhaus, *Nano Today*, 2011, **6**, 401-418.
18. J. Zheng, C. Zhang and R. M. Dickson, *Phys. Rev. Lett.*, 2004, **93**, 077402.
19. T. Udaya Bhaskara Rao and T. Pradeep, *Angew. Chem. Int. Ed.*, 2010, **49**, 3925-3929.
20. J. T. Petty, J. Zheng, N. V. Hud and R. M. Dickson, *J. Am. Chem. Soc.*, 2004, **126**, 5207-5212.
21. H. Kawasaki, H. Yamamoto, H. Fujimori, R. Arakawa, M. Inada and Y. Iwasaki, *Chem. Commun.*, 2010, **46**, 3759-3761.
22. S.-I. Tanaka, J. Miyazaki, D. K. Tiwari, T. Jin and Y. Inouye, *Angewandte Chemie*, 2011, **123**, 451-455.
23. X. Le Guevel, V. Trouillet, C. Spies, G. Jung and M. Schneider, *J. Phys. Chem. C*, 2012, **116**, 6047-6051.
24. T. Yang, Z. Li, L. Wang, C. Guo and Y. Sun, *Langmuir*, 2007, **23**, 10533-10538.
25. D. M. Eby, N. M. Schaeublin, K. E. Farrington, S. M. Hussain and G. R. Johnson, *ACS Nano*, 2009, **3**, 984-994.
26. H. R. Luckarift, M. B. Dickerson, K. H. Sandhage and J. C. Spain, *Small*, 2006, **2**, 640-643.
27. W.-Y. Chen, J.-Y. Lin, W.-J. Chen, L. Luo, E. W.-G. Diau and Y.-C. Chen, *Nanomedicine*, 2010, **5**, 755-764.
28. Y.-H. Lin and W.-L. Tseng, *Anal. Chem.*, 2010, **82**, 9194-9200.
29. T. H. Chen and W. L. Tseng, *Small*, 2012, **8**, 1912-1919.
30. Y. Tao, Y. H. Lin, Z. Z. Huang, J. S. Ren and X. G. Qu, *Adv. Mater.*, 2013, **25**, 2594-2599.
31. J. Xie, Y. Zheng and J. Y. Ying, *J. Am. Chem. Soc.*, 2009, **131**, 888-889.
32. K. Chaudhari, P. L. Xavier and T. Pradeep, *ACS Nano*, 2011, **5**, 8816-8827.
33. L. H. Doerrer, *Dalton Trans.*, 2010, **39**, 3543-3553.
34. A. Sennuga, J. van Marwijk and C. G. Whiteley, *Nanotechnology*, 2012, **23**.
35. T. Teranishi, M. Hosoe, T. Tanaka and M. Miyake, *J. Phys. Chem. B*, 1999, **103**, 3818-3827.
36. J. Zheng, P. R. Nicovich and R. M. Dickson, *Annu. Rev. Phys. Chem.*, 2007, **58**, 409-431.
37. A. Sebetci and Z. B. Guvenc, *Surf. Sci.*, 2003, **525**, 66-84.
38. L. Z. Gao, J. Zhuang, L. Nie, J. B. Zhang, Y. Zhang, N. Gu, T. H. Wang, J. Feng, D. L. Yang, S. Perrett and X. Yan, *Nat. Nanotechnol.*, 2007, **2**, 577-583.
39. C. H. Liu and W. L. Tseng, *Anal. Chim. Acta*, 2011, **703**, 87-93.
40. A. Asati, S. Santra, C. Kaittanis, S. Nath and J. M. Perez, *Angew Chem. Int. Ed.*, 2009, **48**, 2308-2312.
41. W. W. He, Y. Liu, J. S. Yuan, J. J. Yin, X. C. Wu, X. N. Hu, K. Zhang, J. B. Liu, C. Y. Chen, Y. L. Ji and Y. T. Guo, *Biomaterials*, 2011, **32**, 1139-1147.
42. K. Zhang, X. Hu, J. Liu, J. J. Yin, S. Hou, T. Wen, W. He, Y. Ji, Y. Guo, Q. Wang and X. Wu, *Langmuir*, 2011, **27**, 2796-2803.
43. R. W. Bally and T. C. J. Gribnau, *J. Clin. Chem. Clin. Bio.*, 1989, **27**, 791-796.
44. M. Bisaglia, S. Mammi and L. Bubacco, *J. Biol. Chem.*, 2007, **282**, 15597-15605.
45. J. N. Tiwari, K. Nath, S. Kumar, R. N. Tiwari, K. C. Kemp, N. H. Le, D. H. Youn, J. S. Lee and K. S. Kim, *Nat. Commun.*, 2013, **4**.
46. A. Dhakshinamoorthy, S. Navalon, M. Alvaro and H. Garcia, *Chemsuschem*, 2012, **5**, 46-64.

Nanoscale Accepted Manuscript